URBAN AREA APPLICATION AND CALIBRATION OF ALOS/PALSAR FULL POLARIMETRIC OBSERVATION DATA

PI-number: 033
Hajime FUKUCHI
Tokyo Metropolitan University
Asahigaoka 6-6, Hino, Tokyo 191-0065, Japan
Tel: +81-42-585-8660 Fax: +81-42-585-8660
E-mail: fuku@tmu.ac.jp

1. ABSTRACT

We evaluate a polarimetric calibration method in which antenna distortion matrixes and Faraday rotation effect are taken into consideration simultaneously by using PALSAR full polarimetric observation data. As examples of full polarimetric observation data applications in urban areas, we extracted area-averaged orientation angle of artificial structures such as houses and buildings in urban area.

2. POLARIMETRIC CALIBRATION[1]

2.1 Polarimetric Calibration Methods

Several polarimetric calibration techniques, which could attain sufficient calibration result under condition without Faraday Rotation(FR) effect, have been proposed. But those may lead calibration errors in the presence of FR effect. On the other hand, polarimetric calibration technique subject to FR effect has been addressed in several papers, but these method needs measured data in which antenna distortion matrices are calibrated. In polarimetric calibration, it is important to calibrate concisely and precisely with few reference point targets and few suppositions of observation model.

We proposed polarimetric calibration method taking both channel imbalance and crosstalk of receiving and transmitting antennas, and FR effect into consideration using two reference reflectors which are the polarization preserving reflector and polarization rotating one. Then, we apply our calibration method to PALSAR data in order to show the validity of our calibration method. We compare antenna distortion matrix which are derived from our calibration and those derived by JAXA calibration.

2.2 Proposed Calibration Method

We adopted full polarimetric observation model shown in Fig.1. By using two reference reflectors, polarization preserving reflector and polarization rotation one, and assuming that cross-talk factor, C , is small enough, we can derive FR angle, cross-talk factor and channel imbalance factor simultaneously as shown in Fig.1.

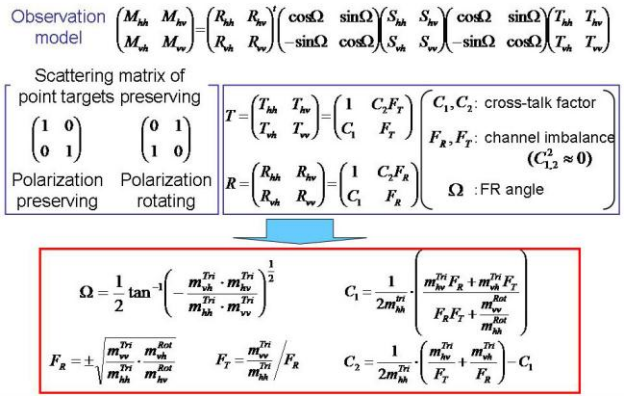

Fig.1 Observation model and calbration algorithm

2.3 Calibration Experiments

We tried calibration experiments as a part of calibration and validation activities of PALSAR carried out under the guidance and leadership of JAXA. We have made 5 measurements from June to October in 2006. We deployed several reference reflectors such as polarization preserving reflector, polarization rotating one and polarization selective one. In this study, we use two reflectors in order to derive both antenna distortion matrices and FR angle simultaneously. Then we use a trihedral reflector as the polarization preserving reflector and twisted reflector as polarization rotating one. Furthermore, we use plate reflector as polarization

preserving which is used for evaluation in order to show the validity of our calibration method.

The observation time of ALOS descending orbit is the daytime in Tokyo, and ascending one is the nighttime. In general, the TEC value of daytime is assumed to be larger than nighttime. Therefore, the influence of FR effect is assumed to be larger in descending orbit measurement. The reflectors were deployed on very large bare ground in suburban area of Musashi-Murayama, Tokyo, which is assumed to be the most suitable for a calibration experiment. Fig. 2 is the PALSAR image of experimental place on October 21 in 2006. Each reflector is deployed over same place in each experiment. We deployed each reflector with enough separation distances more than 100m so that each reflector's response may not interfere with each other. We deployed 8 reflectors in total as shown in Fig.2.

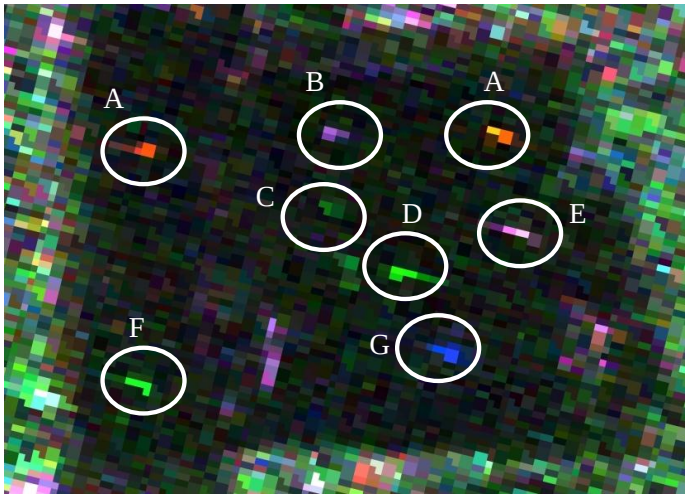

Fig.2 PALSAR image of calibration experiment
A:H-selective B:Trihedral C:Pol-rotating(passive)
D:Pol-rotating(active) E:Plate F:Twisted
G:V-selective
(red:HH, green:HV, blue:VV Oct. 21, 2006)

2.4 Calibration results

A. Antenna Distortion Matirices

In this section, we show polarimetric calibration results using PALSAR data in August and October in 2006. Using the algorithm shown in Fig.1, we derive the antenna distortion matrices of receiving and transmitting antenna. Table 1 shows derived antenna distortion matrices of both produced by JAXA and our calibration results. As we are interested in polarimetric calibration, HV, VH and VV properties are expressed as relative vector values against HH measurement results. JAXA data in Table 1 are derived from PALSAR measurement of Amazon, Rio Branco.

Table 1 Derived antenna distortion matrix of
(a) Receiving and (b) Transmitting antennas
($\angle$ angles in degrees)

(a)	HH/HH	HV/HH	VH/HH	VV/HH
JAXA Calibration	$1\angle 0$	$0.001\angle 131.49$	$0.01\angle 128.12$	$0.722\angle -1.88$
Our Calibration (Aug. 2006)	$1\angle 0$	$0.015\angle 92.11$	$0.025\angle 115$	$0.744\angle -7.62$
Our Calibration (Oct. 2006)	$1\angle 0$	$4.80\times10^{-3}\angle 115$	$2.88\times10^{-2}\angle 97.2$	$0.740\angle 0.411$

(b)	HH/HH	HV/HH	VH/HH	VV/HH
JAXA Calibration	$1\angle 0$	$0.013\angle 79.37$	$0.013\angle -151$	$1.03\angle 21.81$
Our Calibration (Aug. 2006)	$1\angle 0$	$0.021\angle 117$	$0.025\angle 115$	$1.05\angle 29.46$
Our Calibration (Oct. 2006)	$1\angle 0$	$7.06\times10^{-3}\angle 140$	$2.88\times10^{-2}\angle 97.2$	$1.09\angle 25.1$

Note that difference of derived receiving antenna distortion matrix of VV amplitude between our calibration and JAXA calibration is about 0.02, and difference of VV phase between the two is less than 6°. As regards cross talk of HV and VH, the amplitude of those two are almost same level. We suspect the reason why the phase difference in HV and VH between our result and JAXA one is relatively large compared to VV, is due to low signal-to-noise ratio of derived cross talk level. Then these results show that the derived receiving antenna distortion matrix between those two methods is quite similar. Same as receiving antenna, derived

transmitting antenna distortion matrix between those two methods are quite similar.

B. FR angle

Using the algorithm in Fig.1 and iteration process, we derive the one-way FR angle from PALSAR data in August and October in 2006. And then, we compare the derived angle with the calculated FR angle based on Freeman method. It is noted that antenna distortion matrix effect should be removed in advance from measured matrix components. We also calculate the FR angle with another approach, which is Bickel and Bates method. In addition, we calculate theoretical FR angle using Total Electron Content(TEC) value. We used TEC values which are vertically integrated values of observation site. Table 2 shows these FR angles.

Table 2 Calculated one-way FR angles

Calculation equation	2006.8.3	2006.10.21
Theoretical	3.7	6.2
Our method	1.3	5.7
Freeman method	1.8	5.5
Bickel and Bates method	1.6	5.5

The calculated FR angles of our method, Freeman method and Bickel and Bates method are quite similar. On the other hand, theoretically calculated FR angle is larger than estimated FR angles by other three methods. This may be due to difference of calculation region of FR angle, that is, theoretical equation uses TEC value derived from GPS satellite signal whose orbital altitude is relatively high about 20,000km compared to ALOS orbit altitude of 691.65km. Therefore, considering the fact that the TEC value includes the area higher than ALOS altitude, the theoretically calculated FR angle should be larger than FR angles derived from PALSAR observation.

C. Calibrated Plate's Polarization Property

Fig. 3 shows three measured polarization properties of plate, observation value M without calibration, JAXA calibration with FR effect and our calibration with FR effect compensation. Fig.4 also shows the measured co-polarization signatures of plate. These two figures are derived from October 2006 observation. The cross-talk level HV/HH of plate's property calibrated by our method is -39.2dB and VH/HH is -47.9 dB, which are very small levels. Furthermore, the channel imbalance of plate's property calibrated by our method is 1.01. These good results can be also seen in Fig. 4 in which polarization signature of our calibration result shows almost the same as ideal signature. On the other hand, plate's polarization property of JAXA calibration is rather distorted in spite of quite similar property of antenna distortion matrices between our calibration and JAXA calibration, which is mentioned in Table 1. This is due to FR effect which remains in JAXA calibration.

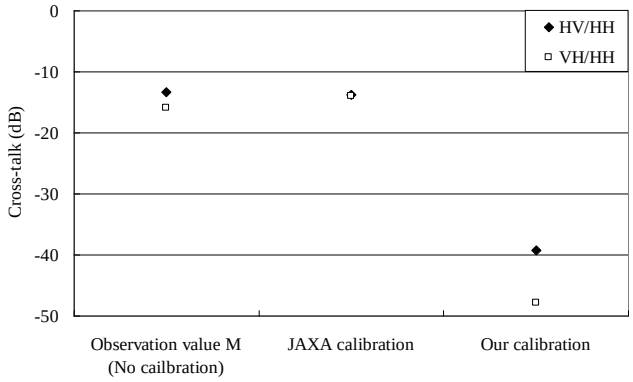

(a)

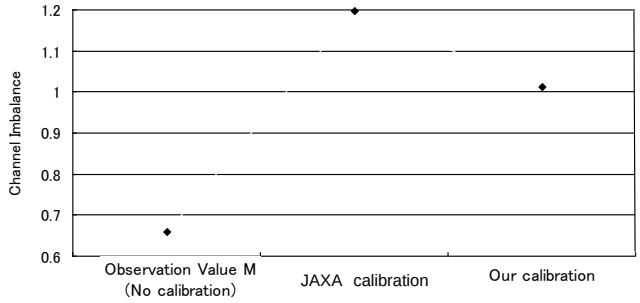

(b)

Fig.3 Cross-talk (a) and channel imbalance(b) levels of the plate reflector

3. URBAN PARAMETER EXTRACTION FROM POLSAR DATA

3.1 Objectives of study

It is very useful to know urban structure parameters, such as size and orientation angle of buildings, even as macroscopic average values over area of concern. By using data analysis using full-polarimetric measurement results, we can derive or estimate such area-averaged urban parameters which can not be observed from simple HH, HV and VV pseudo-color

map due to insufficiency of spatial resolution of POLSAR.

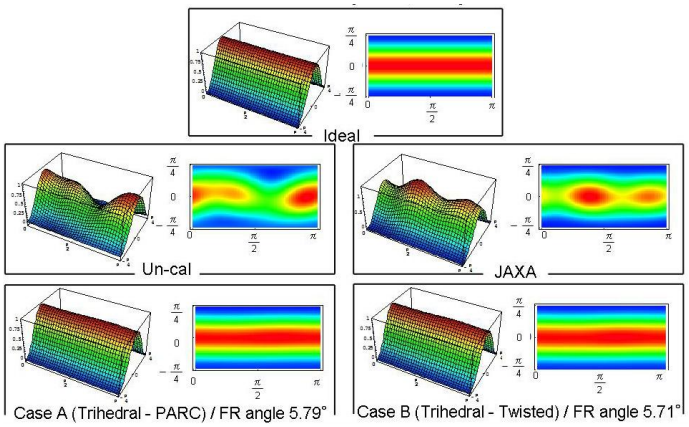

Fig.4 Polarization signature of Plate Reflector

3.2 POLSAR data and Ground-Truth data
We used the following POLSAR measurements over Tokyo urban area;

- PALSAR : L-band, 9-times repeated measurements over the same area during 1.5 year, 2 kinds of azimuth observation directions (Ascending and Descending)
- Pi-SAR : L- and X-band repeated measurements during several years, 3 azimuth observation directions

We also used the following data to assist to obtain ground-truth values regarding area-averaged urban structure parameters;

- 1/2500 buildings POLYGON map: this includes not only buildings size, shape and height information but also classification of land, road, building usage and so on.
- Optical satellite image taken by QuickBird

Fig.5 shows observation example by PALSAR. Figs.6 and 7 show POLYGON map and optical QuickBird map at where we used to extract area averaged structure orientation information in the following sections. They are pictures at the same area of Tachikawa, western part of Tokyo.

3.3 Derivation of structure orientation angle
We aimed to derive urban structure orientation angle objectively from POLYGON data. As shown in Fig.8 , we apply 2-dimensional FFT over the region

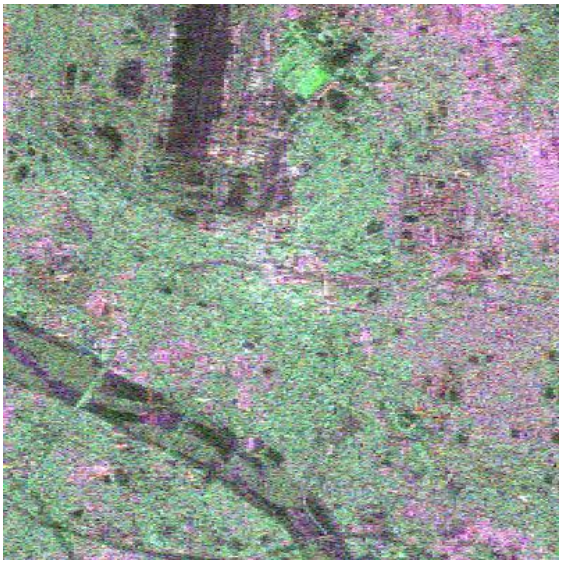

Fig.5 Full polarimetric PALSAR observation

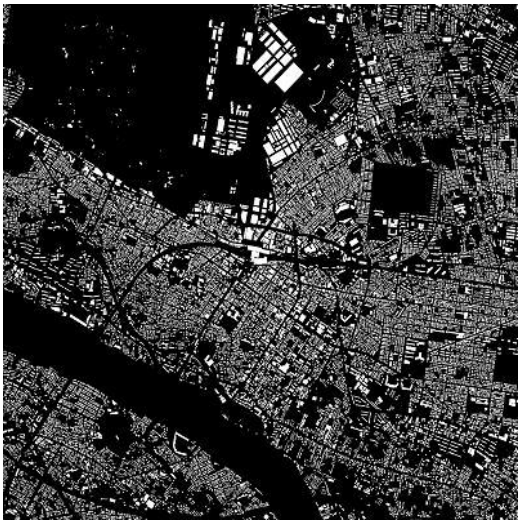

Fig.6 1/2500 POLYGON map

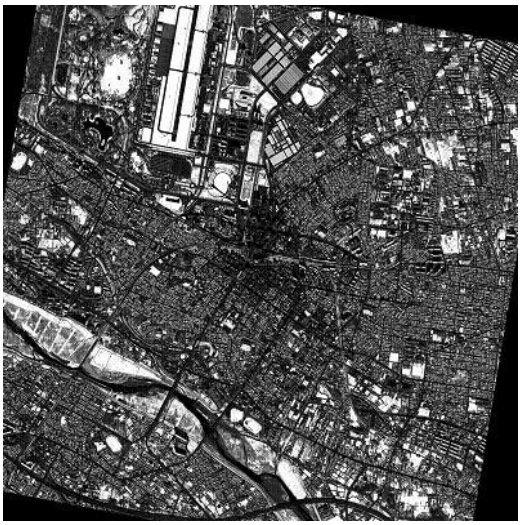

Fig.7 Optical QuickBird observation

of interest and from this spatial spectrum the area-averaged structure orientation angle is extracted as shown in Fig.9. This ground-truth data are derived from many areas in Tachikawa.

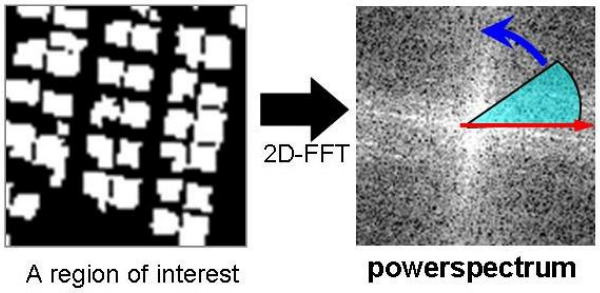

Fig.8 2D-FFT of POLYGON map

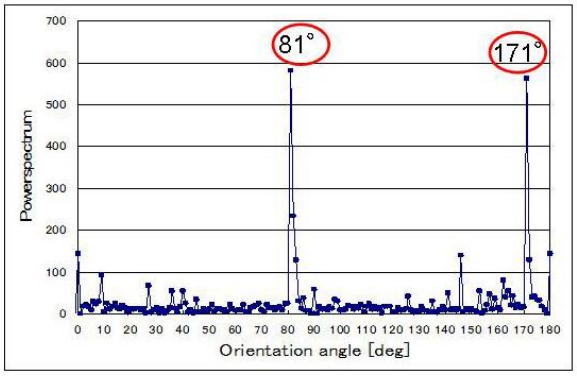

Fig.9 Derivation of structure orientation angles

3.4 POLSAR data analysis

In order to carry out unified analysis using POLSAR data, registration is applied to all POLSAR data into Pi-SAR based observation coordinates. Simultaneously, POLSAR data analysis explained below is done over 10-by-10 pixels. By using knowledge that there is correlation between ground structure orientation angle and argument of complex correlation coefficient, gamma, on circularly polarized POLSAR measurement bases[2], we derive this argument for each area of concern. The definition of this correlation coefficient is shown in Fig.10. The brackets in this equation mean average over the area mentioned in the previous paragraph. The argument, phi, can be derived from components of scattering matrix of linearly polarized POLSAR measurement bases. In the equation, S denotes components of scattering matrix and its suffixes represents components of polarization. The suffixes r and l mean circularly polarized bases and h and v mean linearly polarized ones.

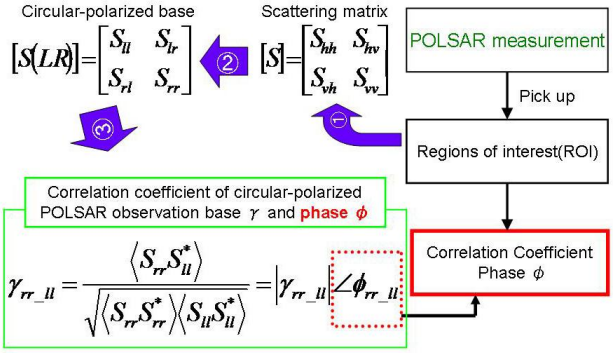

Fig.10 Correlation coefficient of circularly polarized POLSAR observation

Then, from the above procedure, we derived urban structure orientation angle, θ, objectively from POLYGON data using 2-dimensional FFT analysis. Also, we derive argument, ϕ, of correlation coefficient with circularly polarized components which was transformed from observed linearly polarized matrix.

3.5 Example of analysis

In Fig.11, an example of the relation between relations between structure orientation angle theta (abscissa) and argument phi(ordinate) derived from Pi-SAR L-band observation. Although the data scatter to some extent, there are correlation between theta and phi. We extract the median values of phi shown by red points.

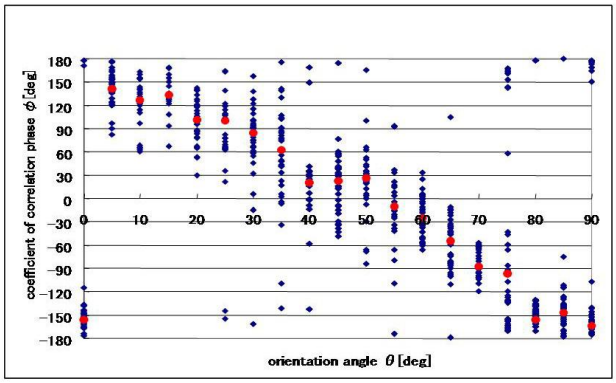

Fig.11 Relation between phi and theta derived from Pi-SAR L-band observation

In Fig.12, median values relations between structure orientation angle and argument phi based on several POLSAR observation including Pi-SAR L-band and

X-band, and PALSAR ascending and descending are shown. In this figure each dot represents the relation derived from one average area. From this figure, clear correlation between orientation angles and arguments is observed even different measurement conditions. This results show similar relations were obtained regardless platforms, orbits and frequencies. Then, for efficient derivation of area-averaged structure orientation angle over wide area, we obtain linear regression relationship. By using this simple linear regression relation, we can estimate area-averaged structure orientation angle over wide area systematically. For example, Fig.13 shows result of this approach on the area shown in Figs.5, 6 and 7. The left map in Fig.13 shows structure orientation map derived POLYGON map and right one shows those derived POLSAR observation.

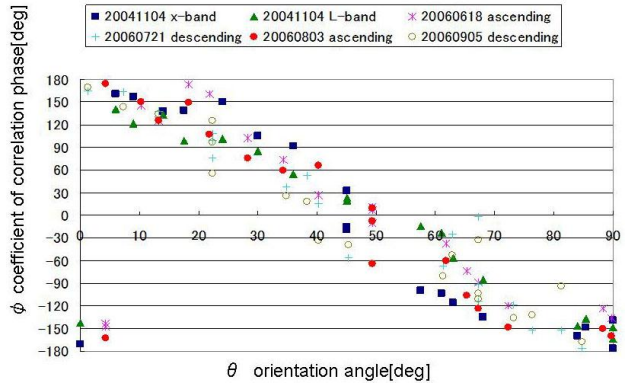

Fig. 12 Relation between orientation angle and POLSAR correlation phase

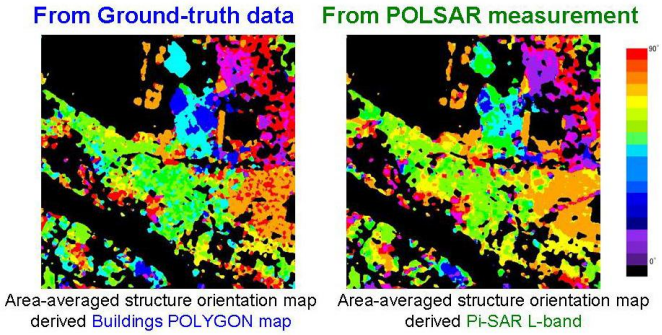

Fig.13 Area averaged structure orientation angle

We cannot estimate the structure orientation angles from Fig.5 because of poor spatial resolution. However, we clearly observe similarity between two orientation maps in Fig.13. Fig.14 shows scatter plot between two figures in Fig.13 in which phi is phase unwrapped. It is also clearly observed that two maps in Fig.13 has good correlation.

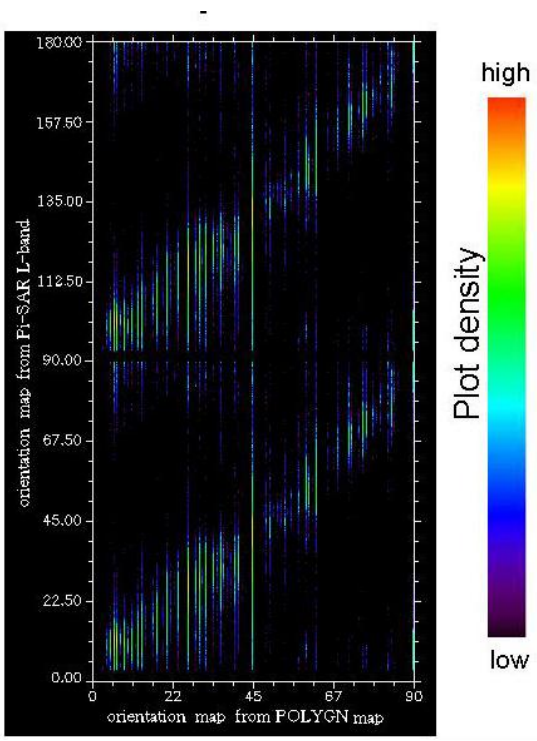

Fig.14 Relation of orientation angles in Fig.13

4. CONCLUSIONS

We proposed polarization calibration methods which can derive both FR angle and antenna distortion matrices simultaneously. We also have shown that area-averaged structure orientation angles relative to incident angle of POLSAR in urban area can be estimated from argument of correlation coefficient of circularly-polarized observation bases. It is quite interesting that by this approach we can estimate area-averaged urban parameters even if we can not distinguish them from conventional received signal component intensity map due to lack of spatial resolution.

We thank MITI, JAXA and NICT for kind consideration and serving several POLSAR measurement data.

5. REFERENCES

[1] A. Takeshiro, T. Furuya and H. Fukuchi, "Verification of polarimetric calibration method including Faraday rotation compensation using PALSAR data," *IEEE Trans. Geoscience and Remote Sensing*, vol.47, no.12, pp. 3960-3968, December 2009.

[2] K. Iribe and M. Sato, "Analysis of polarization orientation angle shifts by artificial structures," *IEEE Trans. Geoscience and Remote Sensing*, vol.45, no.11, pp. 3417-3425, November 2007.